Kinetics and mechanism of the reaction of Cl atoms with HO2 radicals

ARTICLE *in* INTERNATIONAL JOURNAL OF CHEMICAL KINETICS · DECEMBER 2000

Impact Factor: 1.52 · DOI: 10.1002/kin.1026

3 AUTHORS, INCLUDING:

Véronique Riffault
Ecole Nationale Supérieure des Mines de Dou…
46 PUBLICATIONS **254** CITATIONS
SEE PROFILE

Yuri Bedjanian
CNRS Orleans Campus
67 PUBLICATIONS **853** CITATIONS
SEE PROFILE

Kinetics and Mechanism of the Reaction of Cl Atoms with HO_2 Radicals

VÉRONIQUE RIFFAULT, YURI BEDJANIAN, GEORGES LE BRAS

Laboratoire de Combustion et Systèmes Réactifs, CNRS and Université d'Orléans, 45071 Orléans Cedex 2, France

Received 26 September 2000; accepted 18 December 2000

ABSTRACT: The kinetics and mechanism of the reaction Cl + HO_2 → products (1) have been studied in the temperature range 230–360 K and at total pressure of 1 Torr of helium using the discharge-flow mass spectrometric method. The following Arrhenius expression for the total rate constant was obtained either from the kinetics of HO_2 consumption in excess of Cl atoms or from the kinetics of Cl in excess of HO_2: $k_1 = (3.8 \pm 1.2) \times 10^{-11} \exp[(40 \pm 90)/T]$ cm^3 molecule^{-1} s^{-1}, where uncertainties are 95% confidence limits. The temperature-independent value of $k_1 = (4.4 \pm 0.6) \times 10^{-11}$ cm^3 molecule^{-1} s^{-1} at T = 230–360 K, which can be recommended from this study, agrees well with most recent studies and current recommendations. Both OH and ClO were detected as the products of reaction (1) and the rate constant for the channel forming these species, Cl + HO_2 → OH + ClO (1b), has been determined: $k_{1b} = (8.6 \pm 3.2) \times 10^{-11} \exp[-(660 \pm 100)/T]$ cm^3 molecule^{-1} s^{-1} (with $k_{1b} = (9.4 \pm 1.9) \times 10^{-12}$ cm^3 molecule^{-1} s^{-1} at T = 298 K), where uncertainties represent 95% confidence limits.
 Int J Chem Kinet 33: 317–327, 2001

INTRODUCTION

Reaction (1) between Cl atoms and HO_2 radicals has two possible channels:

$$\mathrm{Cl + HO_2 \longrightarrow HCl + O_2} \qquad \Delta H = -53.8 \pm 0.5 \text{ kcal mol}^{-1} \qquad (1a)$$

$$\longrightarrow \mathrm{OH + ClO} \qquad \Delta H = 2.0 \pm 0.5 \text{ kcal mol}^{-1} \qquad (1b)$$

(enthalpy data are from ref. [1]). The HCl-forming pathway (1a) plays an important role in the stratospheric chlorine partitioning by converting active chlorine species (Cl + ClO) to inactive HCl. At altitudes above 40 km, the efficiency of this reaction in the formation of HCl is comparable with that of Cl reaction with methane, the main source of stratospheric HCl.

The kinetics of reaction (1) has been investigated in numerous studies. In the earlier studies, the value of the total rate constant for reaction (1) was determined by relative rate methods [2–5] or was derived from the fitting to a complex mechanism [6,7]. These indirect measurements of k_1 range between 1.9 and 6.8×10^{-11} cm^3 molecule^{-1} s^{-1} at room temperature. The first direct determination of k_1 was reported by Lee and Howard [8], using a discharge-flow system combined with a laser magnetic resonance detection method. Using pseudo-first conditions in excess of Cl atoms over HO_2 radicals, they measured $k_1 = (4.2 \pm 0.7) \times 10^{-11}$ cm^3 molecule^{-1} s^{-1}, independent of temperature in the range 250–420 K. The most recent study by Dobis and Benson [9], where very low pressure reactor combined with mass spectrometric detection of the species was used, supports this value of k_1, giving $k_1 = (4.45 \pm 0.06) \times 10^{-11}$ cm^3 molecule^{-1} s^{-1}, independent of temperature for $T = 243$–368 K. Although the value of the total rate constant of reaction (1) seems to be well established, the existing data for the branching ratio k_{1b}/k_1 are controversial. From the nonobservation of OH radicals as products of reaction

Correspondence to: Y. Bedjanian (bedjanian@cnrs-orleans.fr)

(1), Burrows et al. [4] derived an upper limit of the rate constant for the OH + ClO-forming channel: $k_{1b} \leq 3.0 \times 10^{-13}$ cm^3 molecule^{-1} s^{-1}. Combined with their value of the total rate constant, $k_1 = (4.4 \pm 0.5) \times 10^{-11}$ cm^3 molecule^{-1} s^{-1}, this leads to an upper limit of the branching ratio: $k_{1b}/k_1 \leq 0.008$ at $T = 298$ K. A much higher value for this branching ratio has been measured by Lee and Howard [8] from direct detection of both OH and ClO radicals, formed in reaction (1b). They reported $k_{1b}/k_1 = (1.09 \pm 0.06) \exp[-(478 \pm 17)/T]$ between 250 and 420 K (with $k_{1b}/k_1 \approx 0.22$ at $T = 298$ K). This result was supported by Cattell and Cox [7], who reported $k_{1a} = 4.4 \times 10^{-11}$ cm^3 molecule^{-1} s^{-1} and $k_{1b} = 9.4 \times 10^{-12}$ cm^3 molecule^{-1} s^{-1} at $T = 308$ K, which corresponds to $k_{1b}/k_1 \approx 0.18$. Finally, in the most recent study by Dobis and Benson [9], a lower value, $k_{1b}/k_1 = 0.05 \pm 0.03$ at $T = 243-368$ K, has been reported. Thus, the available measurements of k_{1b}/k_1 range between 0 and 0.22 at $T = 298$ K, whereas current evaluations of the kinetic data for atmospheric modeling [1,10] recommend a value of k_{1b}/k_1 based on the results of ref. [8]. In addition to application to stratospheric modeling, the precise determination of k_{1b}/k_1 is of interest for the accurate determination of the enthalpy of formation of the HO_2 radical from the kinetic equilibrium (e.g., [11]): Cl + HO_2 ↔ OH + ClO. Also, data on the kinetics and mechanism of reaction (1) may be used to model chemical systems used in the laboratory to study kinetics and mechanisms of HOx/ClOx cross reactions. The main motivation for this work was its relation to the ongoing study of the reaction between OH and ClO in this laboratory:

$$\text{OH} + \text{ClO} \longrightarrow \text{HO}_2 + \text{Cl} \qquad (2a)$$

$$\longrightarrow \text{HCl} + \text{O}_2 \qquad (2b)$$

The occurrence of channel (2b) may solve the discrepancy between observed and modeled HCl concentrations, thus altering the stratospheric chlorine partitioning between its active and inactive forms (e.g., [12,13]). Precise kinetic and mechanistic information on reaction (1) is needed prior to studying the OH + ClO reaction, as one of its channels (1b) is the reverse one of reaction (2a) and the second one (1a) leads to HCl formation. Thus, under certain experimental conditions, reaction (1) can influence both the kinetics of OH + ClO reaction as well as the measured yield of HCl.

The present work reports a kinetic and mechanistic study of reaction (1) in the temperature range between 230 and 360 K.

EXPERIMENTAL

Experiments were carried out in a discharge flow reactor using a modulated molecular beam mass spectrometer as the detection method. The reactor consisted in a Pyrex tube (45-cm length and 2.4-cm i.d.) with a jacket for the circulation of the thermostated liquid (ethanol or water). The configuration of the movable triple injector used for the introduction of the reactants into the reactor is shown in Figure 1. In order to reduce the wall loss of active species, the inner surfaces of the reactor and the injector were coated with halocarbon wax.

In most of the experiments, Cl atoms were generated through the fast reaction of hydrogen atoms with Cl_2:

$$\text{H} + \text{Cl}_2 \longrightarrow \text{HCl} + \text{Cl} \qquad (3)$$

$k_3 = (1.7-3.2) \times 10^{-11}$ cm^3 molecule^{-1} s^{-1} [14]

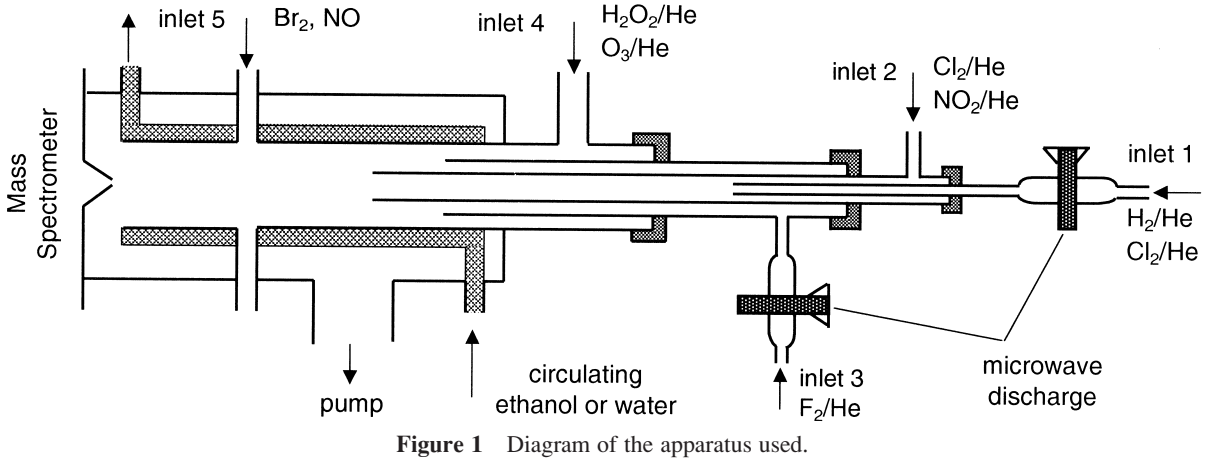

Figure 1 Diagram of the apparatus used.

H atoms were produced by passing a 0.1–1% H_2/He mixture through a microwave discharge, He being used as the carrier gas in all the experiments. The microwave discharge of 0.1–1% Cl_2/He mixture was also used to produce Cl atoms. The net fraction of dissociated Cl_2 was in the range 10–30%. Cl atoms were detected at their parent peak (Cl^+, $m/e = 35$) and also as BrCl at $m/e = 116$, after scavenging by Br_2 at the end of the reactor (Br_2 was added through inlet 5, located 5 cm upstream of the sampling cone) through the reaction:

$$Cl + Br_2 \longrightarrow BrCl + Br \qquad (4)$$

$k_4 = 2.3 \times 10^{-11} \exp[-135/T]$ cm^3 molecule^{-1} s^{-1} [15]

The advantage of the last procedure of Cl detection was to avoid any complication in the direct detection of Cl (at its parent peaks, $m/e = 35/37$) arising from the contribution of both Cl_2 and HCl due to their fragmentation in the ion source of the mass spectrometer (operating at 25–30 eV). Absolute concentrations of Cl atoms could be obtained from the fraction of Cl_2 dissociated in the microwave discharge ($[Cl] = 2\Delta[Cl_2]$) or consumed in reaction (3) with H atoms ($[Cl] = \Delta[Cl_2]$), and also from the fraction of Br_2 consumed in reaction (4): $[Cl] = [BrCl] = \Delta[Br_2]$). The results obtained with these methods were always consistent within a few percent.

The fast reaction of fluorine atoms with H_2O_2 (inlet 4) was used as the source of HO_2 radicals, F atoms being produced in a microwave discharge of F_2/He mixture (inlet 3):

$$F + H_2O_2 \longrightarrow HO_2 + HF \qquad (5)$$

$k_5 = 5.0 \times 10^{-11}$ cm^3 molecule^{-1} s^{-1} ($T = 300$ K) [16]

It was verified by mass spectrometry that more than 90% of F_2 was dissociated in the microwave discharge. To reduce F atom reaction with the glass surface inside the microwave cavity, a ceramic (Al_2O_3) tube was inserted at this part of the injector. H_2O_2 was always used in excess over F atoms. This source of HO_2 radicals is known to produce other active species than HO_2. First, OH radicals can be formed in the reaction of F atoms with H_2O (from H_2O_2):

$$F + H_2O \longrightarrow OH + HF \qquad (6)$$

$k_6 = 1.4 \times 10^{-11} \exp[(0 \pm 200)/T]$cm^3 molecule^{-1} s^{-1} [1]

Other active species that can enter the reactor are O atoms — from the discharge of F_2 or from the secondary reaction $F + OH \rightarrow O + HF$. However, the concentrations of these trace species can be easily measured by adding Br_2 into the reactor. Br_2, being unreactive toward HO_2 radicals, removes all other trace active species coming from the source of HO_2, OH, O, and F atoms (if not completely consumed in reaction with H_2O_2) via the fast reactions:

$$OH + Br_2 \longrightarrow Br + HOBr \qquad (7)$$

$k_7 = 1.8 \times 10^{-11} \exp(235/T)$ cm^3 molecule^{-1} s^{-1} [17]

$$O + Br_2 \longrightarrow BrO + Br \qquad (8)$$

$k_8 = 1.8 \times 10^{-11} \exp(40/T)$ cm^3 molecule^{-1} s^{-1} [18]

$$F + Br_2 \longrightarrow FBr + Br \qquad (9)$$

$k_9 = 2.2 \times 10^{-10}$ cm^3 molecule^{-1} s^{-1} ($T = 300$ K) [19]

Consequently, HOBr, BrO, and FBr can be detected (at $m/e = 96$, 95, and 100, respectively) and quantified by mass spectrometry. HO_2 radicals were detected at their parent peak at $m/e = 33$ (HO_2^+). Their signals were always corrected for the contribution of H_2O_2 due to the fragmentation of H_2O_2 in the ion source. These corrections could be easily done by simultaneous detection of the signals from H_2O_2 at $m/e = 33$ and 34 and were around 10% of the signals corresponding to the initial concentrations of HO_2. In a few experiments, where low concentrations of HO_2 needed to be detected in presence of high H_2O_2 concentrations (branching ratio measurements, see the following), a more complex procedure of HO_2 detection was employed. When NO is added at the end of the reactor (through inlet 5), HO_2 is converted to NO_2 by reaction (10) and can be detected at $m/e = 46$ as NO_2^+:

$$HO_2 + NO \longrightarrow OH + NO_2 \qquad (10)$$

$k_{10} = 3.5 \times 10^{-12} \exp(250/T)$ cm^3 molecule^{-1} s^{-1} [1]

This reaction leads to the simultaneous production of OH radicals, which can be rapidly scavenged by Br_2 (if added simultaneously with NO) through reaction (7), forming HOBr. Assuming stoichiometric conversion of HO_2 to NO_2 (OH) and OH to HOBr, one has $[HO_2] = [NO_2] = [HOBr]$. In a recent work from this laboratory [20], these three methods of HO_2 detection (as HO_2^+, NO_2^+, and $HOBr^+$) were verified to give the same results for experimental concentrations of HO_2. Absolute concentrations of HO_2 were measured using chemical conversion of HO_2 to NO_2 through reaction (10). In order to prevent the possible HO_2 regeneration in reaction (11), calibration experiments were carried out in the presence of Br_2 in the reactor:

$$OH + H_2O_2 \longrightarrow HO_2 + H_2O \quad (11)$$

$$k_{11} = 2.9 \times 10^{-12} \exp(-160/T) \text{ cm}^3 \text{ molecule}^{-1} \text{ s}^{-1} \text{ [1]}$$

Thus, OH was rapidly consumed by Br_2 through reaction (7).

Absolute concentrations of HOBr were measured using the reaction of OH radicals with excess Br_2 [reaction (7)]. OH radicals were formed through the fast reaction of H atoms with excess NO_2:

$$H + NO_2 \longrightarrow OH + NO \quad (12)$$

$$k_{12} = 4 \times 10^{-10} \exp(-340/T) \text{ cm}^3 \text{ molecule}^{-1} \text{ s}^{-1} \text{ [1]}$$

Thus, HOBr concentrations were determined from the consumed fraction of $[Br_2]$: $[OH] = [HOBr] = \Delta[Br_2]$. The possible influence of secondary chemistry on this procedure of absolute calibration of HOBr (and OH) signals was discussed in details in previous articles [17,21].

ClO radicals, which were found as the products of reaction (1), were detected at their parent peak (ClO^+, $m/e = 51$). Reaction (13), converting ClO radicals into the stable species NO_2, was used for the determination of the absolute concentrations of these radicals:

$$ClO + NO \longrightarrow Cl + NO_2 \quad (13)$$

$$k_{13} = 6.4 \times 10^{-12} \exp(290/T) \text{ cm}^3 \text{ molecule}^{-1} \text{ s}^{-1} \text{ [1]}$$

ClO radicals, needed for these calibration experiments, were produced through reaction (14) between ozone and excess Cl atoms:

$$Cl + O_3 \longrightarrow ClO + O_2 \quad (14)$$

$$k_{14} = 2.9 \times 10^{-11} \exp(-260/T) \text{ cm}^3 \text{ molecule}^{-1} \text{ s}^{-1} \text{ [1]}$$

All the other relevant species were detected at their parent peaks: $m/e = 38$ (F_2^+), 70 (Cl_2^+), 36 (HCl^+), 160 (Br_2^+), 30 (NO^+), 46 (NO_2^+), 34 ($H_2O_2^+$). The procedure for the determination of the absolute concentrations of H_2O_2 in the reactor consisted in a chemical titration of H_2O_2/H_2O mixtures by an excess of F atoms and was discussed in details in a previous article from this laboratory [20]. The concentrations of the other stable species in the reactor were calculated from their flow rates obtained from the measurements of the pressure drop in calibrated volume flasks with the species diluted in helium.

The purities of the gases used were as follows: He > 99.9995% (Alphagaz) was passed through liquid nitrogen traps; H_2 > 99.998% (Alphagaz); Cl_2 > 99% (Ucar); Br_2 > 99.99% (Aldrich); F_2 (5% in Helium, Alphagaz); NO_2 > 99% (Alphagaz); NO > 99% (Alphagaz), purified by trap-to-trap distillation in order to remove NO_2 traces. A 70% H_2O_2 solution was purified to around 90% by continuous flowing of helium through the bubbler with H_2O_2. Ozone was produced by an ozonizer (Trailigaz) and was collected and stored in a trap containing silica gel at $T = 195$ K. The trap was pumped before use in order to reduce the O_2 concentration. The resulting oxygen concentration was always <20% of the ozone concentration introduced into the reactor.

RESULTS

Total Rate Constant of the Cl + HO_2 Reaction

Two series of experiments were performed to measure the total rate constant of the reaction Cl + HO_2: one by monitoring HO_2 consumption kinetics in excess of Cl atoms and the other one by monitoring Cl decays in excess of HO_2 radicals.

HO_2 Kinetics in Excess of Cl Atoms. In this series of experiments, reaction (1) has been studied under pseudo-first-order conditions using an excess of Cl atoms over HO_2 radicals. Experiments were carried out in the temperature range 230–360 K. The initial concentration of HO_2 was $(2.5–7.0) \times 10^{11}$ molecule cm^{-3}; the range of Cl concentrations is shown in Table I. The concentrations of the precursors of the reactants, H_2O_2 and Cl_2, in the reactor were $(3–9) \times 10^{11}$ and $\approx 2 \times 10^{13}$ molecule cm^{-3}, respectively. Linear flow velocities were in the range 1450–2100 cm s^{-1}. The consumption of the excess reactant, Cl atoms, was negligible in most of the experiments, although significant (up to 20%) in a few kinetic runs. In this case,

Table I Experimental Conditions and Results for the Study of the Cl + HO_2 Reaction: Kinetics of HO_2 Consumption in Excess of Cl Atoms

Number of Decays	T(K)	[Cl][a]	k_1[b]
12	360	0.8–8.8	4.7 ± 0.6
8	320	0.5–15.3	4.3 ± 0.5
9	300	0.6–12.8	4.4 ± 0.5
8	275	0.4–12.5	4.3 ± 0.5
8	250	0.4–8.4	4.8 ± 0.6
8	230	0.4–7.4	4.8 ± 0.5

[a] Units of 10^{12} molecule cm^{-3}.

[b] Units of 10^{-11} cm^3 $molecule^{-1}$ s^{-1}; errors are 95% confidence limits and include estimated systematic uncertainties.

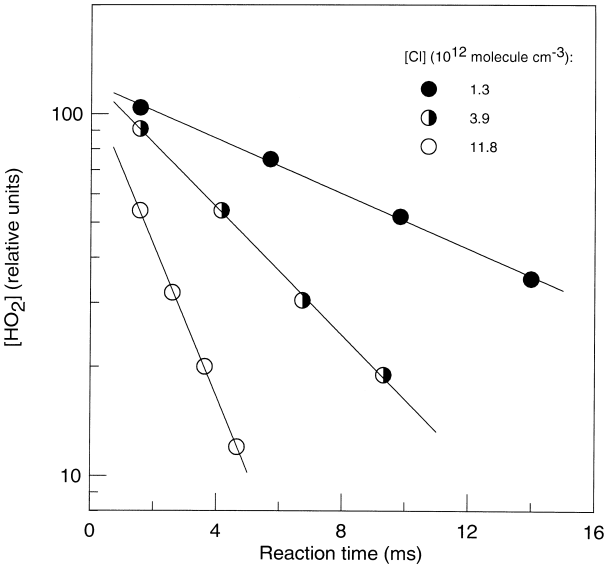

Figure 2 Reaction Cl + HO_2 → products (1): example of kinetic runs of HO_2 consumption in reaction with excess Cl atoms: $T = 300$ K.

the consumption of Cl was taken into account using the mean Cl concentration over the whole reaction time for the calculation of k_1. An example of a kinetic run of the exponential decay of [HO_2] measured with different excess concentrations of Cl atoms is shown in Figure 2. Pseudo-first-order rate constants, $k_1' = -d(\ln[HO_2])/dt$, obtained from such HO_2 kinetics, were corrected for axial and radial diffusion of HO_2 [22]. The diffusion coefficient of HO_2 in He was calculated from that of O_2 in He [23]. The maximal correction on measured values of k_1' was ~10%. Concerning the possible impact of the secondary and side reactions, the most important reactions that could affect the HO_2 kinetics under the experimental conditions used are reaction (15) between Cl and H_2O_2 (precursor of HO_2 radicals) and reaction (16) between OH and HO_2:

$$Cl + H_2O_2 \longrightarrow HO_2 + HCl \qquad (15)$$

$k_{15} = 1.1 \times 10^{-11} \exp(-980/T)$ cm^3 $molecule^{-1}$ s^{-1} [1]

$$OH + HO_2 \longrightarrow H_2O + O_2 \qquad (16)$$

$k_{16} = 4.8 \times 10^{-11} \exp(250/T)$ cm^3 $molecule^{-1}$ s^{-1} [1]

The first of these reactions could lead to the formation of HO_2 and the second one to its consumption. OH radicals are products of reaction (1), and they can be also formed in the source of HO_2 radicals by reaction (6) between F atoms and H_2O. In order to verify the possible influence of these processes on the results, the numerical simulation of the experimental HO_2 decays was carried out with a reaction mechanism including reactions (15) and (16) as well as other processes occurring in this chemical system (e.g., see Table II). The initial concentrations of OH radicals (from the source of HO_2) needed for the calculations could be measured by scavenging OH radicals with excess Br_2 with subsequent detection of HOBr (as explained in the previous section). These concentrations were found to be in the range $(1-2) \times 10^{11}$ molecule cm^{-3} under the experimental conditions of the study. For the branching ratio of the OH-forming channel of reaction (1), the value from this study was used. The originally measured values of k_1' as well as those resulting from the simulation procedure are presented in Figure 3 as a function of Cl atom concentration. It can be noticed that corrections on k_1' are negligible at high values of k_1' and are more important at lower k_1'. This effect is mainly due to the relatively high initial concentration of OH, coming from the HO_2 source, which makes the rate of HO_2 consumption in reaction (16) comparable with that in reaction (1) at low concentrations of Cl atoms. One can note also that the slope of the linear fit to the points in Figure 3, which in fact provides the value of the rate constant for reaction (1), is not significantly affected by the corrections on the individual data points. For example, the difference between the values of k_1 resulting from the two fits presented in Figure 3 is ~5%. Similar corrections were obtained at

Table II Measurements of the Rate Constant of the Reaction Cl + HO_2 → OH + ClO (1b): Mechanism Used for the Modeling of Cl, HO_2, ClO, and OH Experimental Profiles

Reaction	Rate Constant[a] (cm^3 $molecule^{-1}$ s^{-1})
$Cl + H_2O_2 \rightarrow HO_2 + HCl$	$1.1 \times 10^{-11} \exp(-980/T)$
$Cl + HO_2 \rightarrow HCl + O_2$	$(1 - \alpha) \times k_1$[b]
$Cl + HO_2 \rightarrow ClO + OH$	$\alpha \times k_1$
$OH + H_2O_2 \rightarrow HO_2 + H_2O$	$2.9 \times 10^{-12} \exp(-160/T)$
$OH + HO_2 \rightarrow H_2O + O_2$	$4.8 \times 10^{-11} \exp(250/T)$
$OH + HCl \rightarrow Cl + H_2O$	$2.6 \times 10^{-12} \exp(-350/T)$
$OH + Cl_2 \rightarrow Cl + HOCl$	$1.4 \times 10^{-12} \exp(-900/T)$
$ClO + OH \rightarrow Cl + HO_2$	$1.1 \times 10^{-11} \exp(120/T)$
$ClO + HO_2 \rightarrow HOCl + O_2$	$4.8 \times 10^{-13} \exp(700/T)$
ClO + wall → loss	$(1-2)$ s^{-1}
OH + wall → loss	$(3-10)$ s^{-1}
Cl + wall → loss	$(1-3)$ s^{-1}
HO_2 + wall → loss	$(4-10)$ s^{-1}

[a] All rate constants are from [1], except for the wall loss rates measured in this work.

[b] Varied parameters: k_1 = total rate constant of reaction (1) and $\alpha = k_{1b}/k_1$, branching ratio for (1b) channel.

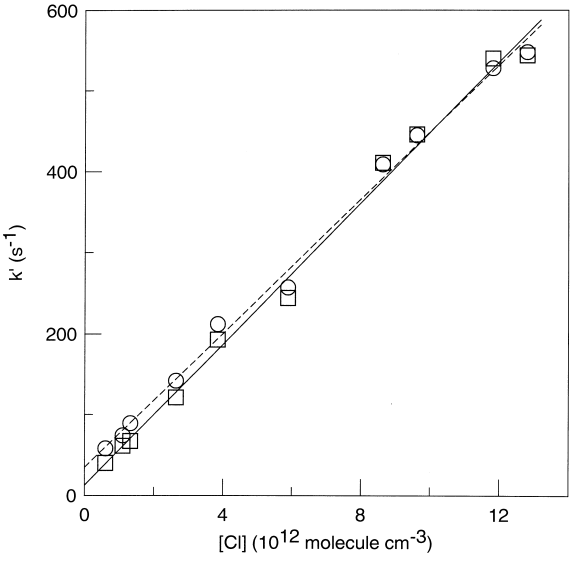

Figure 3 Example of pseudo-first-order plot of HO_2 consumption in reaction with excess Cl atoms at $T = 300$ K: circles—data obtained from the simple exponential fit to experimental kinetics; squares—corrected data, from the simulation of the experimental kinetics using complete mechanism (see text).

the other temperatures of the study. All the results obtained for k_1 in this series of experiments are reported in Table I.

Cl Atom Kinetics in Excess of HO_2. In this series of experiments, in order to measure the rate constant of reaction (1), Cl atom decay kinetics was monitored in the presence of excess HO_2. The initial concentration of Cl atoms (detected as BrCl, see the Experimental section) was $(1.5–2.5) \times 10^{11}$ molecule cm^{-3}; the range of the HO_2 concentrations is presented in Table III. Concentrations of the excess precursor species, Cl_2 and H_2O_2, in the reactor were $(2–3) \times 10^{12}$ and $\approx 1 \times 10^{13}$ molecule cm^{-3}, respectively. The flow velocity in the reactor was 1370–1920 cm s^{-1}. The concentrations of Cl atoms and HO_2 radicals were simultaneously measured as a function of reaction time. A consumption of the excess reactant, HO_2, was also observed (up to 40% in a few kinetic runs). This HO_2 consumption was due to reaction (1), the wall loss of HO_2 radicals, their disproportionation reaction (17), and reactions (16) and (18) with OH and ClO, the products of channel (1b):

$$HO_2 + HO_2 \longrightarrow H_2O_2 + O_2 \qquad (17)$$

$$k_{17} = 2.3 \times 10^{-13} \exp(600/T) \text{ cm}^3 \text{ molecule}^{-1} \text{ s}^{-1} \quad [1]$$

$$HO_2 + ClO \longrightarrow HOCl + O_2 \qquad (18)$$

Table III Experimental Conditions and Results for the Study of the Cl + HO_2 Reaction: Kinetics of Cl Consumption in Excess of HO_2

Number of Decays	T (K)	$[HO_2]^a$	$k_1{}^b$
9	340	1.0–5.0	4.0 ± 0.7
8	299	0.6–3.9	4.1 ± 0.6
7	260	0.3–3.6	4.0 ± 0.6
10	240	0.2–3.2	4.3 ± 0.6

[a] Units of 10^{12} molecule cm^{-3}.

[b] Units of 10^{-11} cm^3 $molecule^{-1}$ s^{-1}; errors are 95% confidence limits and include estimated systematic uncertainties.

$$k_{18} = 4.8 \times 10^{-13} \exp(700/T) \text{ cm}^3 \text{ molecule}^{-1} \text{ s}^{-1} \quad [1]$$

Two approaches to calculate the rate constant were used to take into account this HO_2 consumption. First, the HO_2 concentration was considered as constant and the mean value of this concentration along the kinetic run was used in calculations of k_1. Second, the value of the rate constant k_1 was derived from the simulation of Cl decay kinetics using experimentally measured HO_2 profiles and a simple two-step mechanism, including reaction (1), and the combined loss of Cl atoms on the wall and in reaction with H_2O_2 (with the rate 5–9 s^{-1} in the temperature range of the study). The values of k_1 resulting from these two approaches were consistent within 5%. The examples of the pseudo-first-order plots measured from Cl atom decay kinetics are shown in Figure 4. The pseudo-first-order rate constant values were corrected to take into ac-

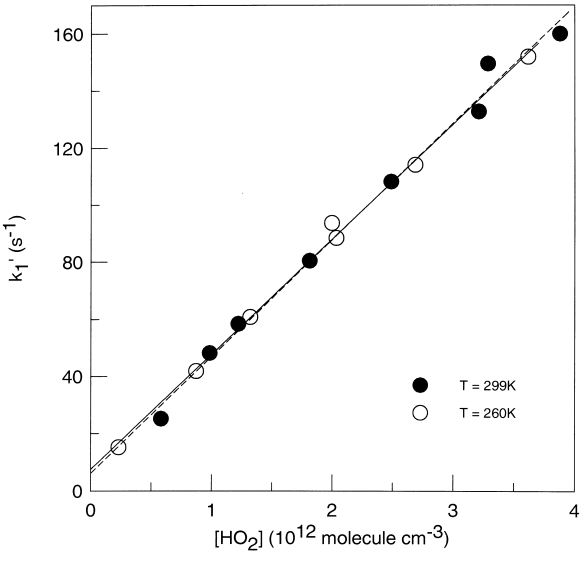

Figure 4 Example of pseudo-first-order plots of consumption of Cl atoms in reaction with excess HO_2: dashed and continuous lines represent linear fit to experimental points at $T = 299$ and 260 K, respectively.

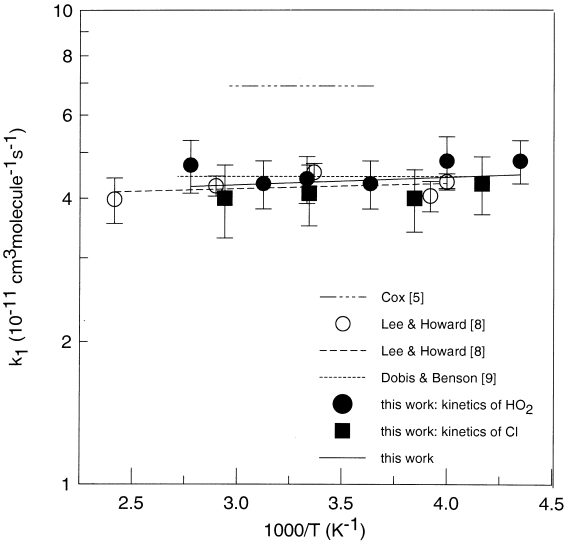

Figure 5 Temperature dependence of the total rate constant of the reaction Cl + HO_2 ⟶ products.

count the axial and radial diffusion of Cl atoms. The diffusion coefficient of Cl in He was calculated from D_{Ar-He} [23]. The corrections were within 5%. The intercepts in Figure 4, 6–8 s^{-1}, are in good agreement with the Cl loss rate measured in the absence of HO_2. This relatively low rate of Cl consumption in the absence of HO_2 (F_2 discharge off) shows a negligible contribution of reaction (15) to the Cl consumption rate compared with that in reaction (1). Another secondary reaction, which could potentially influence the kinetics of Cl atoms, is reaction (19) between OH and Cl_2, leading to the regeneration of Cl:

$$OH + Cl_2 \longrightarrow Cl + HOCl \qquad (19)$$

$$k_{19} = 1.4 \times 10^{-12} \exp(-900/T) \text{ cm}^3 \text{ molecule}^{-1} \text{ s}^{-1} \text{ [1]}$$

However, the contribution of this reaction was negligible, considering the relatively low value of k_{19}, the relatively low concentration of Cl_2 in the reactor [$(2-3) \times 10^{12}$ molecule cm^{-3}], and the fact that OH is only a minor product of reaction (1), which, in addition, reacts rapidly with HO_2. Results for k_1 from this series of experiments are reported in Table III. These results are in good agreement with those obtained from HO_2 decay kinetics in excess of Cl. All the results for k_1 from the present work are shown in Figure 5 together with the data obtained in previous temperature-dependent studies of reaction (1) [5,8,9]. The continuous straight line in Figure 5, resulting from the least-squares analysis of the present data, provides the following Arrhenius expression:

$$k_1 = (3.8 \pm 1.2) \times 10^{-11} \exp[(40 \pm 90)/T] \text{ cm}^3 \text{ molecule}^{-1} \text{ s}^{-1} \quad T = 230-360 \text{ K}$$

The quoted uncertainties represent 2σ.

Rate Constant of the ClO- and OH-forming Channel of Reaction (1)

In this series of experiments on the determination of the rate constant of reaction (1b), Cl atoms and H_2O_2 molecules were used as initial reactants. Reaction Cl + H_2O_2 leads to the formation of HO_2 radicals, which, in turn, react with Cl atoms through reaction (1). An example of the kinetic runs observed in this chemical system is presented in Figure 6. As one could expect, steady state for HO_2 concentration was observed [due to HO_2 formation and rapid consumption in reactions (15) and (1), respectively]. Both OH and ClO were observed as the products formed in this chemical system. The continuous curves in Figure 6 show the results of the numerical simulation, with the complete reaction mechanism given in Table II. Two parameters were varied: the total rate constant of reaction (1) and the branching ratio for channel (1b). For the example presented in Figure 6, the best fit was obtained with $k_1 = (4.0 \pm 0.2) \times 10^{-11}$ cm^3 molecule^{-1} s^{-1} and $k_{1b}/k_1 = 0.22 \pm 0.01$ (uncertainties represent calculation accuracy only). This value of k_1

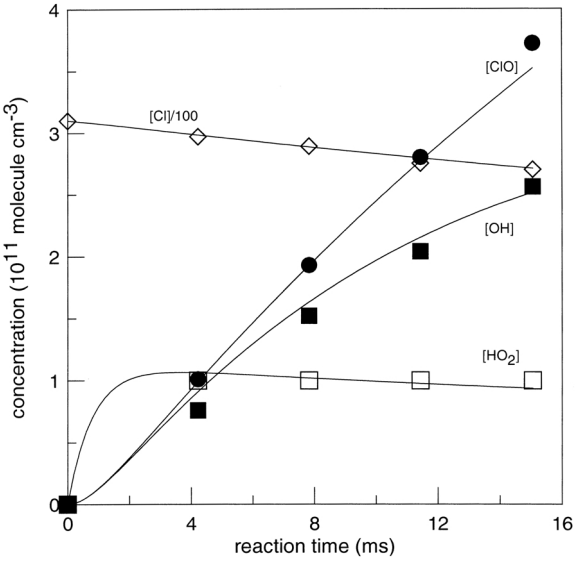

Figure 6 Example of experimental (points) and simulated (solid lines) kinetics for the species detected in Cl + H_2O_2 chemical system: Initial concentrations of reactants: [Cl] = 3.1×10^{13} and [H_2O_2] = 1.1×10^{13} molecule cm^{-3}. Best fit was obtained with $k_1 = (4.0 \pm 0.2) \times 10^{-11}$ cm^3 molecule^{-1} s^{-1} and $k_{1b}/k_1 = 0.22 \pm 0.01$.

Table IV Experimental Conditions and Results for the Study of the Reaction Cl + HO_2 → ClO + OH (1b): Kinetics of the ClO Formation

T(K)	Number of Experiments	$[Cl]_0 \times 10^{-13}$[a]	$[HO_2]_{ss} \times 10^{-11}$[a,b]	$k_{1b} \times 10^{12}$[c]
360	6	1.4–4.4	1.0–7.7	13.8 ± 3.1
330	6	1.5–4.0	1.1–4.1	11.2 ± 2.3
295	6	2.4–5.1	0.6–2.6	9.9 ± 2.8
273	5	1.2–2.9	0.8–3.1	7.8 ± 1.5
250	7	1.9–4.7	0.5–3.0	5.6 ± 1.0
230	5	1.0–5.0	0.7–2.0	5.1 ± 1.3

[a] Concentrations are in molecule cm^{-3} units.
[b] Mean steady-state concentration of HO_2 along the reaction zone.
[c] Units of cm^3 $molecule^{-1}$ s^{-1}; uncertainties represent 95% confidence limits and include estimated systematic uncertainties.

agrees well with the direct measurements (see the preceding), although its strong dependence on the rate constant of reaction (15), as well as on the accuracy of $[H_2O_2]$ measurements, should be noted. Two observations can be made from Figure 6. First, for reaction time $t > 2$ ms, where changes in [Cl] and $[HO_2]$ are not significant, almost linear kinetics of ClO formation could be observed, according to the equation $d[ClO]/dt = k_{1b}[HO_2][Cl]$. The deviation of OH kinetics from that of ClO shows that the influence of secondary reactions on OH kinetic profiles is significant. In order to reduce the influence of possible secondary reactions on the results of the measurements, only kinetics of ClO formation was used for the determination of k_{1b}. Furthermore, HO_2 source reaction (15) was excluded from the mechanism used in the simulation, and the rate constant of channel (1b) was derived from the best fit to ClO kinetics using the experimental profiles of [Cl] and $[HO_2]$. All the simulations were carried out for reaction time >3 ms, where steady-state concentrations of HO_2 were achieved. Kinetics of ClO were found to be defined mainly by reaction (1b) and were not sensitive to secondary ClO reactions. The changes in k_{1b} due to the introduction of ClO secondary reactions (see Table II) into the simulation model were <10%. Experimental conditions and results obtained for k_{1b} are reported in Table IV. The concentrations of HO_2 given in this table represent the mean steady-state HO_2 concentration along the reaction zone. The steady-state concentrations of HO_2 depended mainly on the concentration of H_2O_2 in the reactor, which was varied in the range $(0.6–5.2) \times 10^{13}$ molecule cm^{-3}. The independence of the values found for k_{1b} (e.g., see Table V, where results obtained for k_{1b} at $T = 360$ K are detailed) on the concentrations of the reactants Cl and HO_2, which were widely varied ([Cl] up to 5 times and $[HO_2]$ up to 7.7 times), confirms that ClO radicals originate from

Table V Experimental Conditions and Results for the Study of the Reaction Cl + HO_2 → ClO + OH (1b) at T = 360 K

Expt. No.	$[HO_2]_{ss} \times 10^{-11}$[a,b]	$[Cl]_0 \times 10^{-13}$[a]	$k_{1b} \times 10^{12}$[c]
1	1.0	2.3	13.2 ± 0.4
2	2.2	0.9	15.0 ± 0.4
3	2.5	1.6	15.1 ± 0.4
4	2.7	4.7	13.1 ± 1.0
5	3.6	2.1	12.8 ± 0.6
6	7.7	1.9	13.3 ± 0.6

[a] Concentrations are in molecule cm^{-3} units.
[b] Mean steady-state concentration of HO_2 along the reaction zone.
[c] Units of cm^3 $molecule^{-1}$ s^{-1}; uncertainty is 2σ from the precision of the fit.

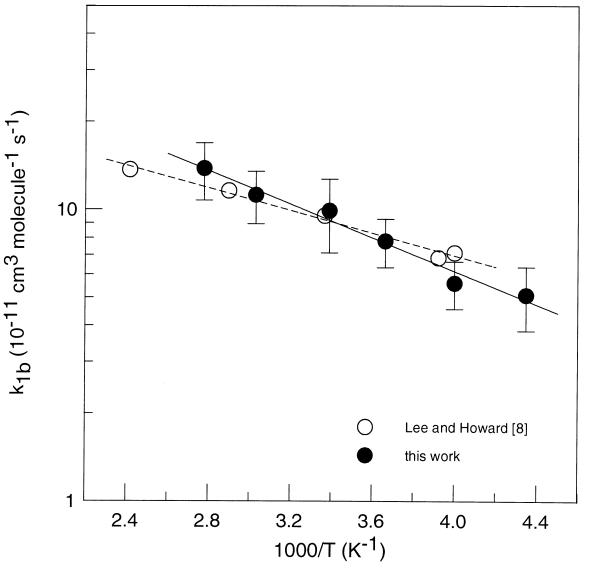

Figure 7 Temperature dependence of the rate constant for the OH + ClO-forming channel of reaction (1).

Table VI Summary of Data for the Rate Constant of the Reaction Cl + HO_2 → Products (1)

T (K)	P (Torr)	k_1[a]	Technique[b]	Method[c]	Reference
295	1–2	$1.9^{+2.9}_{-1.2}$[d]	DF/MS	R	Leu and DeMore [2]
306	760	2.5 ± 1.0[e]	FP/UV	R	Cox and Derwent [6]
298	0.24–0.36	6.8 ± 2.5	DF/MS	R	Poulet et al. [3]
298	~2	4.4 ± 1.5[d]	DF/LMR	R	Burrows et al. [4]
274–338	760	6.0 ± 3.0[d]	FP/UV	R	Cox [5]
250–414	0.9–1.5	4.2 ± 0.7	DF/LMR	D	Lee and Howard [8]
308	50–760	$4.4^{+4.4}_{-2.2}$	FP/UV	R	Cattell and Cox [7]
243–368	~0.001	4.45 ± 0.06	VLPR/MS	D	Dobis and Benson [9]
230–360	~1	4.4 ± 0.6	DF/MS	D	This work

[a] Units of 10^{-11} cm^3 molecule^{-1} s^{-1}; uncertainty as quoted by authors.

[b] DF = discharge flow, FP = flash photolysis, VLRP = very low pressure reactor, MS = mass spectrometry, UV = UV absorption spectroscopy, LMR = laser magnetic resonance.

[c] R = relative measurements or from fitting to a complex mechanism, D = direct measurements.

[d] Updated according to currently recommended data for the reference reactions Cl + H_2O_2 and Cl + H_2 [1].

[e] This value was revised in [5] to be >4.0.

reaction (1b). The temperature dependence of k_{1b} is shown in Figure 7. It provides the following Arrhenius expression:

$$k_{1b} = (8.6 \pm 3.2) \times 10^{-11} \exp[-(660 \pm 100)/T] \text{ cm}^3 \text{ molecule}^{-1} \text{ s}^{-1} \quad T = 230\text{–}360 \text{ K}$$

where the quoted uncertainties represent 2σ.

The approach used for the detection of the low concentrations of OH and HO_2 in the preceding experiments needs to be discussed. In fact, the mass spectrometric detection of small amounts of OH and HO_2, especially in the presence of high concentrations of H_2O_2 and H_2O (from H_2O_2), represents a significant experimental challenge, owing to the decomposition of H_2O_2 and H_2O in the ion source of the mass spectrometer, leading to the high contribution of these species to the signals at $m/e = 33$ (HO_2^+) and $m/e = 17$ (OH^+). In order to avoid these complications in the present experiments, Br_2 (~10^{14} molecule cm^{-3}) was added at the end of the reactor (see the Experimental section). Consequently, OH radicals were converted to HOBr and were detected as $HOBr^+$ at $m/e = 96$. For HO_2 detection, NO was added together with Br_2 at the end of the reactor. This led to the chemical conversion of HO_2 to OH through reaction (10), followed by OH conversion to HOBr [through reaction (7)]. The concentrations of HOBr detected in this case correspond to the sum of [HO_2] and [OH]. The addition of Br_2 led also to the conversion of Cl atoms into BrCl [via reaction (4)], which allowed Cl detection as $BrCl^+$ at $m/e = 116$. This procedure was more convenient than the direct Cl detection at $m/e = 35/37$ (Cl^+), where contributions from Cl_2 and HCl should be taken into account. The method used for the detection of OH and HO_2 seems to be correct, especially considering (1) the independence of k_{1b} on the concentrations of the reactants and (2) the fact that OH, HO_2, and ClO kinetics could be well fitted with the same parameters (k_1 and k_{1b}).

DISCUSSION

A very weak negative temperature dependence of the rate constant of the Cl + HO_2 reaction was observed in the present study: $k_1 = (3.8 \pm 0.6) \times 10^{-11} \exp[(40 \pm 90)/T]$ cm^3 molecule^{-1} s^{-1}. In fact, considering the experimental uncertainty, the temperature-independent value of k_1 can be recommended:

$$k_1 = (4.4 \pm 0.6) \times 10^{-11} \text{ cm}^3 \text{ molecule}^{-1} \text{ s}^{-1} \quad T = 230\text{–}360 \text{ K}$$

All the results for k_1 from the previous studies are reported in Table VI for comparison. The value from this work is in excellent agreement with the results from two previous temperature-dependent studies [8,9]. In fact, Lee and Howard [8] have also observed a very weak negative temperature dependence of the rate constant: $k_1 = (3.87 \pm 0.54) \times 10^{-11} \exp[(25 \pm 42)/T]$ cm^3 molecule^{-1} s^{-1}. Their $k_1(T)$ data points, shown in Figure 5, are undistinguishable from the present results.

Table VII reports all the available experimental data on reaction (1b). The present result for k_{1b} is in good agreement with that obtained by Lee and Howard [8]. Although somewhat different Arrhenius expressions for k_{1b} were obtained in these two studies, the results of the individual measurements of k_{1b} at dif-

Table VII Summary of Data for the Rate Constant of the Reaction Cl + HO_2 → OH + ClO (1b)

T (K)	k_{1b} (cm^3 molecule^{-1} s^{-1})	Technique[a]	Reference
298	$< 3 \times 10^{-13}$	DF/LMR	Burrows et al. [4]
250–414	$4.1 \times 10^{-11} \exp(-450/T)$ $(9.1 \pm 1.3) \times 10^{-12}$ (T = 298 K)	DF/LMR	Lee and Howard [8]
308	$9.4^{+9.4}_{-4.7} \times 10^{-12}$	FP/UV	Cattell and Cox [7]
243–368	$(2.2 \pm 1.4) \times 10^{-12}$	VLPR/MS	Dobis and Benson [9]
230–360	$8.6 \times 10^{-11} \exp(-660/T)$ $(9.4 \pm 1.9) \times 10^{-12}$ (T = 298 K)	DF/MS	This work

[a] DF = discharge flow, FP = flash photolysis, VLRP = very low pressure reactor, MS = mass spectrometry, UV = UV absorption spectroscopy, LMR = laser magnetic resonance.

ferent temperatures agree well (see Figure 7). The upper limit of 3×10^{-13} cm^3 molecule^{-1} s^{-1} reported for k_{1b} by Burrows et al. [4] is about 30 times lower than the value of k_{1b} measured in the present work and in ref. [8]. This upper limit was derived from the nonobservation of OH radicals, their concentration being considered as steady state, defined by OH formation and consumption in reactions (1b) and (11), respectively. The possible reasons for the very low concentrations of OH under the experimental conditions of that study were discussed in ref. [8]. The value of k_{1b} measured in the most recent study [9] by Dobis and Benson is also significantly lower than that of Lee and Howard [8] and the present one. In order to explain the discrepancy between their result and that of Lee and Howard, Dobis and Benson [9] suggested two possible reasons, which could lead to an overestimation of k_{1b} under the experimental conditions of ref. [8]: first, some extra HO_2 formation (which was not taken into account in the calculation of the branching ratio) in reaction (15) and, second, additional ClO formation in the sequence of reactions (20) and (21):

$$Cl + O_2 + M \longrightarrow ClO_2 + M \qquad (20)$$

$k_{20} = 2.7 \times 10^{-33} (T/300)^{-1.5}$ cm^6 molecule^{-2} s^{-1} [1]

$$Cl + ClO_2 \longrightarrow ClO + ClO \qquad (21)$$

$k_{21} = 1.2 \times 10^{-11} \exp[(0 \pm 250)/T]$ cm^3 molecule^{-1} s^{-1} [1]

Concerning this last point, it should be noted that most of the results in [8] were obtained with OH, but not with ClO detection. The values of k_{1b} determined in the present study support the measurements of Lee and Howard, although they were obtained in a completely different way. In fact, these authors used the titration of initial concentration of HO_2 by an excess of Cl atoms with subsequent measurements of the OH or ClO yield. This procedure led to the determination of the branching ratio for OH- and ClO-forming channel of reaction (1). In the present work, another approach was used: the rate constant k_{1b} was directly determined from the kinetics of ClO formation, which was observed simultaneously with temporal profiles of both reactants, Cl and HO_2. Moreover, the value of k_{1b}, found in this way, was independent of the concentrations of the reactants (which were widely varied), confirming that ClO radicals originated from the reaction between Cl and HO_2.

In addition to kinetic parameters, thermochemical data can also be obtained from the present study since reaction (1b) is reversible:

$$Cl + HO_2 \longleftrightarrow OH + ClO \qquad (1b,2a)$$

Using the activation energies for forward and reverse reactions, one can determine the reaction enthalpy change and, subsequently, the enthalpy of formation of HO_2 radicals (using known heats of formation for other species involved in the equilibrium): $\Delta H_r = E_{forward} - E_{reverse}$. Using $E_{forward} = (1.3 \pm 0.2)$ kcal mol^{-1} from this work, $E_{reverse} = -(0.6 \pm 0.2)$ kcal mol^{-1} from two recent studies of the reaction (2) [13,24], enthalpy data from ref. [1]: $\Delta H_{f,298} = 28.9$, 9.3, and 24.4 kcal mol^{-1} for Cl, OH, and ClO, respectively, we obtain: $\Delta H_r = (1.9 \pm 0.4)$ kcal mol^{-1} and $\Delta H_{f,298}(HO_2) = (2.9 \pm 0.4)$ kcal mol^{-1}. This latter value is in good agreement with the current NASA panel recommendation (2.8 ± 0.5) kcal mol^{-1} [1] and is somewhat lower than that recommended by IUPAC [10]: 3.5 kcal mol^{-1}.

Current evaluations of the kinetic data for use in stratospheric modeling [1,10] recommend the values of k_1 and k_{1b}, which are based on the results of ref. [8]. The present study supports these recommended values.

This study has been carried out within a project funded by the European Commission through the "Environment and Climate" Programme (contract "COBRA"–ENV–CT97–0576). Stéphane Lelièvre is gratefully acknowledged for participation in some of the experiments.

BIBLIOGRAPHY

1. De More, W. B.; Sander, S. P.; Golden, D. M.; Hampson, R. F.; Kurylo, M. J.; Howard, C. J.; Ravishankara, A. R.; Kolb, C. E.; Molina, M. J. Chemical Kinetics and Photochemical Data for Use in Stratospheric Modeling; NASA, JPL, California Institute of Technology: Pasadena, CA, 1997.
2. Leu, M.-T.; Demore, W. B. Chem Phys Lett 1976, 41, 121.
3. Poulet, G.; Le Bras, G.; Combourieu, J. J Chem Phys 1978, 69, 767.
4. Burrows, J. P.; Cliff, D. I.; Harris, G. W.; Thrush, B. A.; Wilkinson, J. P. T. Proc R Soc London A 1979, 368, 463.
5. Cox, R. A. Int J Chem Kinet 1980, 12, 649.
6. Cox, R. A.; Derwent, R. G. J Chem Soc, Faraday Trans 1 1977, 73, 272.
7. Cattell, F. C.; Cox, R. A. J Chem Soc, Faraday Trans 2 1986, 82, 1413.
8. Lee, Y.-P.; Howard, C. J. J Chem Phys 1982, 77, 756.
9. Dobis, O.; Benson, S. W. J Am Chem Soc 1993, 115, 8798.
10. Atkinson, R.; Baulch, D. L.; Cox, R. A.; Hampson, R. F.; Kerr, J. A.; Rossy, M. J.; Troe, J. J Phys Chem Ref Data 1997, 26, 521.
11. Hills, A. J.; Howard, C. J. J Chem Phys 1984, 81, 4458.
12. Toumi, R.; Bekki, S. Geophys Res Lett 1993, 20, 2447.
13. Lipson, J. B.; Elrod, M. J.; Beiderhase, T. W.; Molina, L. T.; Molina, M. J. J Chem Soc, Faraday Trans 1997, 93, 2665.
14. Westley, F.; Herron, J.; Frizzell, D.; Hampson, R.; Mallard, G. NIST Chemical Kinetics Data Base, version 17-2Q98, NIST Standard Reference Data, Gaithersburg, MD, 1998.
15. Bedjanian, Y.; Laverdet, G.; Le Bras, G. J Phys Chem A 1998, 102, 953.
16. Walther, C. D.; Wagner, H. G. Ber Bunsenges Phys Chem 1983, 87, 403.
17. Bedjanian, Y.; Le Bras, G.; Poulet, G. Int J Chem Kinet 1999, 31, 698.
18. Nicovich, J. M.; Wine, P. H. Int J Chem Kinet 1990, 22, 379.
19. Bemand, P. P.; Clyne, M. A. A. J Chem Soc, Faraday Trans 2 1976, 72, 191.
20. Bedjanian, Y.; Riffault, V.; Le Bras, G.; Poulet, G. J Phys Chem 2001, 105, 573.
21. Bedjanian, Y.; Le Bras, G.; Poulet, G. J Phys Chem 1999, 103, 7017.
22. Kaufman, F. J Phys Chem 1984, 88, 4909.
23. Marrero, T. R.; Mason, E. A. J Phys Chem Ref Data 1972, 1, 3.
24. Kegley-Owen, C. S.; Gilles, M. K., Burkholder, J. B.; Ravishankara, A. R. J Phys Chem 1999, 103, 5040.